

## Investigation of bonding in the solid state using experimental charge density\*

G.U. KULKARNI

Chemistry and Physics of Materials Unit, Jawaharlal Nehru Centre for Advanced Scientific Research, Jakkur, Bangalore 560 064.

### Abstract

A method of investigating chemical bonding in crystalline solids using experimental charge density is presented. A refinement procedure based on multipole formalism for X-ray diffraction data has been described along with topographical analysis of charge distribution. The method has been applied to a study of  $\alpha$  and  $\beta$  polymorphs of *p*-nitrophenol and their photochemical activity. Besides revealing many structural differences, the study has brought out significant differences in intra- and intermolecular regions of the two forms as seen from deformation density maps. Relief maps of the negative Laplacians in the plane of intermolecular hydrogen bonds show polarization of the oxygen lone-pair electrons towards hydrogen. Charge appears to migrate from the benzene ring region of the molecule to nitro and hydroxyl groups as the structure changes from  $\beta$  to  $\alpha$  form. On prolonged irradiation of the  $\alpha$  form, charge migrates in the opposite way resembling more like charge distribution in light stable  $\beta$  form. Molecular dipole moments in solid state are found to be considerably larger than the value in the free molecule.

**Keywords:** Crystal structure, charge density, *p*-nitrophenol, polymorphism, photoirradiation.

### 1. Introduction

Experimental charge density method using X-diffraction to study chemical bonding in solid state is becoming increasingly popular amongst chemists in recent years.<sup>1,2</sup> The model is based on a promolecular density obtained as a superposition of the spherical atomic densities centered at nuclear positions. The promolecule can serve as a reference state relative to which charge migration due to bond formation takes place. In order to visualize charge distribution due to chemical bond formation, a refinement formalism based on nucleus-centered multipole expansion of the electron density is commonly used.<sup>3</sup> Accordingly, aspherical atomic density is described in terms of spherical harmonics.

$$\rho_{\text{atom}}(r) = \rho_{\text{core}}(r) + \rho_{\text{valence}}(r) + \rho_{\text{def}}(r).$$

Thus, for each atom,

$$\rho_{\text{atom}}(r) = \rho_{\text{core}}(r) + P_v \kappa^3 \rho_{\text{valence}}(\kappa r) + \sum_{l=0} \kappa^3 R_l(\kappa' \zeta r) \sum_{m=0} \sum_{p=\pm 1} P_{\text{imp}} Y_{\text{imp}}(\theta, \varphi)$$

with the origin at the atomic nucleus. The population coefficients,  $P_{\text{imp}}$ , are refined along with  $\kappa$  and  $\kappa'$  parameters which control the radial dependence of the valence shell. Quantitative analysis of the electronic structure may be carried out by using critical point (CP) search method developed by Bader.<sup>4</sup> The set of CPs in  $\rho(r)$  at  $r_c$  is defined such that  $\nabla \rho(r_c) = 0$ . The

\*Text of lecture delivered at the Annual Faculty Meeting of the Jawaharlal Nehru Centre for Advanced Scientific Research at Bangalore on November 13, 1998.

value of  $\rho_e$  in a bond measures its strength; the trace of diagonalised Hessian at  $r_e$  (the Laplacian),  $\nabla^2\rho_e$ , measures the extent of depletion and contraction of charges, and ellipticity,  $\epsilon$ , obtained as ratios of the Hessian eigenvalues perpendicular to the bond minus one, measures the degree of planarity or conjugation. The position of CP in a bond gives an idea of polarity of the bond. CP tends to shift closer to the more electropositive atom and therefore the polarity of the bond,  $\nabla$ , may be expressed as the percentage shift of CP from mid-point of the bond, normalized with half of the bond length. The vertical displacement,  $d$ , of CP from the line joining bonded atoms measures the extent of bending of the bonding orbitals.

In the last few years, there have been a number of charge density studies on materials of interest in quantum chemistry and medicine. Wozniak *et al.*<sup>5</sup> examined attractive inter- and intramolecular N...O interactions in N, N-dipicrylamine and its ionic complexes. Topological analysis of the charge distribution in maleate salts<sup>6,7</sup> has shown that short hydrogen bonds possess some covalent character. Charge density studies on L-dopa,<sup>8</sup> Vitamin C<sup>9</sup> and DL-aspartic acid<sup>10</sup> have been reported recently. Some workers have analysed non-centrosymmetric crystals of importance in nonlinear optics.<sup>11, 12</sup> Coppens *et al.*<sup>13</sup> carried out charge density studies on long-lived metastable excited states in nitrosyl complexes using synchrotron radiation.

We have initiated a research program recently to investigate charge density in a variety of materials. Our efforts in this direction began with a study of organic crystals in relation to chemical reactivity and polymorphic form.<sup>14, 15</sup> We chose *p*-nitrophenol for this purpose. The  $\alpha$  form is known to undergo a topochemically controlled photochemical transformation, manifesting itself in an irreversible color change of the crystal from yellow to red. The origin of the color change is however not clear and could be due to a side reaction. The  $\beta$  modification is light stable at room temperature. Thus, *p*-nitrophenol provides an interesting example of polymorphism where one polymorph is thermodynamically unstable and the other is photochemically unstable. Previously, some efforts were made to explain this phenomenon based on crystal structure analysis,<sup>16, 17</sup> and ENDOR measurements.<sup>18</sup> However, the results are not conclusive. We have carried a detailed investigation on  $\beta$  and  $\alpha$  polymorphs of *p*-nitrophenol using charge density method, having collected high-resolution X-ray diffraction data at low temperatures on both the forms as well as on irradiated crystal of  $\alpha$  form. Our study has shown differences in the molecular structure in  $\beta$  and  $\alpha$  forms, particularly in the hydrogen bond region and more importantly, significant differences in charge densities and associated properties of the two forms.

## 2. Experimental

Pale yellow crystals of  $\beta$  and  $\alpha$  forms were grown from aqueous and benzene solutions, respectively. High-quality crystals of the two modifications were chosen after detailed examination under optical microscope. X-ray diffraction intensities were measured by  $\omega$  scans using Siemens three-circle diffractometer attached with a CCD area detector and a graphite monochromator for MoK $\alpha$  radiation (50kV, 40mA). The crystals were cooled on the diffractometer using a stream of cold nitrogen gas from a vertical nozzle and were held at 110K throughout data collection. Extra care was taken not to expose the  $\alpha$  crystal to light for extended hours during the experiment.

**Table 1**  
Crystal data and experimental details

Chemical formula	C <sub>6</sub> H <sub>2</sub> NO <sub>3</sub>		
Formula weight	139.11		
Cell setting	Monoclinic		
	$\beta$	$\alpha$	Irradiated $\alpha$
Space group	P2 <sub>1</sub> /n	P2 <sub>1</sub> /c	P2 <sub>1</sub> /c
a (Å)	3.6812(3)	6.1664(1)	6.1414(1)
b (Å)	11.1152(9)	8.8366(3)	8.8032(2)
c (Å)	14.6449(12)	11.5435(4)	11.5013(2)
$\beta$ (°)	92.804(2)	103.390(1)	103.338(1)
D <sub>x</sub> (mg m <sup>-3</sup> )	1.544	1.510	1.527
Radiation type	Mo K $\alpha$		
Wave length (Å)	0.71073		
No of reflections for cell parameters	9874	10029	9880
$\mu$ (mm <sup>-1</sup> )	0.13	0.12	0.13
Temperature (K)	110		
Crystal form	Needle	Rectangular block	Rectangular block
Crystal size (mm)	0.4 × 0.32 × 0.28	0.3 × 0.2 × 0.14	0.3 × 0.23 × 0.15
Crystal color	Pale yellow	Pale yellow	Red
Data collection	Siemens CCD		
Diffractometer	$\phi$ scan		
Data collection	4.0		
Crystal-detector distance (cm)	9874		
No. of measured reflections	4603	10029	9880
No. of independent reflections	4459	4147	4684
No. of observed reflections	0.035	4045	5476
$R_{\text{merge}}$	0.035	0.033	0.04
$R_{\text{int}}$	0.035	0.035	0.044
$\theta_{\text{max}}$ (°)	49.93	49.61	49.61
( $\sin \theta / \lambda$ ) <sub>max</sub>	1.08	1.07	1.07
Range of h, k, l	-7 → h → 7	-10 → h → 11	-10 → h → 11
	-23 → k → 16	-18 → k → 13	-18 → k → 13
	-28 → l → 15	-23 → l → 15	-23 → l → 15
Refinement (multipole and kappa)			
Refinement on F			
	R	0.025	0.022
	wR	0.032	0.029
	S	1.89	1.80
No. of reflections used in the refinement	4459	4045	5476
No of parameters used	303	303	303
$N_{\text{ref}}/N_p$	14.8	13.4	19.7
H-atom treatment	see text		
Weighting scheme	$w = 1/\sigma^2(F) = (4F^2)/\sigma^2(F^2)$		
	$\sigma^2(F^2) = \sigma^2_{\text{counting}}(F^2) + P^2(F^4)$		
(Shift/e.s.d.) <sub>max</sub>	0.06	0.01	0.02
$\Delta\rho_{\text{max}}$ (eÅ <sup>-3</sup> )	0.12	0.07	0.17
$\Delta\rho_{\text{min}}$ (eÅ <sup>-3</sup> )	-0.10	-0.11	-0.19

Table II

Analysis of the bond critical points for the irradiated  $\alpha$  (top row),  $\alpha$  (middle row) and  $\beta$  (bottom row) forms

Bond	$\rho$	$\nabla^2\rho$	$\epsilon$	$\Delta\%$	$d$
C(1)—C(2)	2.11(3)	-18.1(1)	0.28	8.8C(2)	0.021
	2.08(5)	-18.1(1)	0.27	1.5 C(2)	0.011
	2.21(5)	-22.4(2)	0.26	5.6 C(2)	0.014
C(2)—C(3)	2.19(3)	-19.8(1)	0.21	2.1C(3)	0.015
	2.09(5)	-18.0(1)	0.22	1.3 C(3)	0.005
	2.20(5)	-21.7(1)	0.24	4.0 C(2)	0.009
C(3)—C(4)	2.05(3)	-17.5(1)	0.22	2.5C(4)	0.013
	2.01(5)	-17.8(1)	0.21	5.3 C(3)	0.012
	2.24(5)	-23.0(2)	0.18	12.7 C(3)	0.016
C(4)—C(5)	2.14(3)	-18.9(1)	0.26	2.1C(4)	0.018
	2.20(5)	-19.4(1)	0.22	1.1 C(5)	0.014
	2.34(6)	-23.4(2)	0.19	5.1 C(5)	0.019
C(5)—C(6)	2.10(3)	-20.8(1)	0.22	12.8C(6)	0.018
	2.10(5)	-18.0(1)	0.18	3.9 C(5)	0.007
	2.35(6)	-24.2(2)	0.17	0.3 C(6)	0.018
C(6)—C(1)	2.17(3)	-21.6(1)	0.27	4.1C(1)	0.009
	2.04(5)	-18.4(1)	0.24	6.4 C(6)	0.008
	2.27(6)	-22.3(2)	0.22	6.4 C(6)	0.013
C(2)—H(2)	1.87(5)	-17.1(1)	0.04	23.1H(2)	0.021
	1.89(4)	-21.0(1)	0.07	20.0 H(2)	0.017
	1.89(5)	-16.6(2)	0.04	23.9 H(2)	0.015
C(3)—H(3)	1.88(6)	-18.5(2)	0.09	30.3H(3)	0.006
	1.97(4)	-20.2(1)	0.10	24.6 H(3)	0.007
	2.01(4)	-19.0(2)	0.12	20.9 H(3)	0.015
C(5)—H(5)	1.93(5)	-20.1(1)	0.09	18.1H(5)	0.002
	1.97(4)	-20.3(1)	0.06	18.5 H(5)	0.007
	1.96(4)	-19.9(2)	0.09	18.5 H(5)	0.014
C(6)—H(6)	1.85(5)	-17.1(1)	0.09	24.0H(6)	0.007
	1.82(3)	-17.7(1)	0.13	20.0 H(6)	0.017
	1.96(4)	-19.6(2)	0.14	19.3 H(6)	0.015
O(1)—C(1)	2.12(5)	-17.5(2)	0.13	17.4C(1)	0.027
	2.09(6)	-21.1(3)	0.05	22.9 C(1)	0.027
	2.32(6)	-20.0(3)	0.04	35.4 C(1)	0.022
O(1)—H(1)	2.40(10)	-42.4(7)	0.04	55.9H(1)	0.020
	2.91(6)	-45.2(6)	0.09	46.5 H(1)	0.041
	2.68(11)	-36.4(4)	0.14	47.7 H(1)	0.026
N—C(4)	1.80(3)	-12.3(1)	0.22	19.1C(4)	0.006
	1.78(5)	-14.0(2)	0.29	25.5 C(4)	0.016
	1.91(5)	-12.5(2)	0.20	17.2 C(4)	0.018
O(2)—N	3.15(6)	-2.3(2)	0.16	4.5N	0.004
	3.49(8)	-8.7(3)	0.14	2.1 N	0.009
	3.14(14)	2.5(4)	0.08	1.8 N	0.025
O(3)—N	3.18(6)	3.3(2)	0.12	1.2O(3)	0.006
	3.39(8)	5.0(3)	0.20	0.6 O(3)	0.006
	3.03(2)	10.6(5)	0.25	0.6 N	0.031

$\rho_c$  ( $e\text{\AA}^{-3}$ ) is the electron density at the critical point ( $\nabla\rho(r_c)=0$ ),  $\nabla^2\rho_c$  ( $e\text{\AA}^{-3}$ ) the Laplacian (trace of the diagonalised Hessian);  $\epsilon$  the ellipticity (ratio of the Hessian eigenvalues perpendicular to the bond minus one);  $\Delta$  the bond polarity (percentage shift of the CP from mid-point of the bond, normalized with half of the bond length);  $d$  ( $\text{\AA}$ ) the perpendicular distance between the critical point and the internuclear vector.

Initially, unit cell parameters and orientation matrix of the crystal were determined using ~60 reflections from 25 frames collected over a small  $\omega$  scan of 7.5°. A hemisphere of reciprocal space was then collected in two shells using SMART software<sup>19</sup> with  $2\theta$  settings of the detector at 32° and 70°. The coverage was found to be ~92% using ASTRO routine.<sup>20</sup> Data reduction was performed using SAINT program<sup>19</sup> and orientation matrix along with detector and cell parameters were refined for every 40 frames on all the measured reflections (Table I). As preliminary check on the X-ray intensity data, crystal structures of the polymorphs were re-determined using SHELXTL program<sup>20</sup> and were compared with the reported structures.<sup>16,17</sup>

As a first step towards charge density analysis, a high-order refinement of the data was carried out using reflections with  $\sin\theta/\lambda \geq 0.85 \text{ \AA}^{-1}$  and  $F_o \geq 10\sigma$ . The positions of H atom were found using difference Fourier method and were adjusted to theoretical values (C—H, 1.085 Å; O—H, 0.96 Å) and were held constant throughout refinement along with their isotropic temperature factors. As usual, the nonhydrogen atoms were treated anisotropically. These served as initial parameters for multipolar refinement.

Multipolar refinement for charge density analysis was carried out using XDLSM routine of the XD package.<sup>21</sup> The nonhydrogen atoms were refined up to octapole moments while the hydrogen atoms were restricted to quadrupole moments. Charge neutrality constraint was applied to the molecule through all cycles of refinement.  $r$ -factors showed significant improvement over conventional refinement from around 6% to ~2%.  $\kappa$  refinement was also carried out following which the residual index showed marginal improvement. XDPROP routine was used to calculate total electron density  $\rho(r)$ , deformation density  $\Delta\rho$  and Laplacian  $\nabla^2\rho$  (Table II).

Charge density analysis of the intermolecular hydrogen contacts was carried out using PARST<sup>22</sup> and XD programs (Table III). Pseudoatomic charges and dipole moments obtained using XDPROP are listed in Table IV.

### 3. Results and discussion

#### 3.1. Structures of $\beta$ and $\alpha$ forms

In Fig. 1 we show the molecular packing diagrams of  $\beta$  and  $\alpha$  forms, respectively. The molecular structure differs in the two forms to some extent. We find that OH and NO<sub>2</sub> groups are not coplanar with benzene rings in both the forms, the constituent atoms of the two groups showing noticeable displacements above and below the mean plane of the benzene ring. In  $\beta$  form, N atom remains in the mean plane while O(3), O(1) and H(1) atoms show small displacements of -0.08, 0.05 and -0.03 Å, respectively. O(2) atom of the nitro group shows the largest displacement of 0.22 Å from the benzene mean plane. In  $\alpha$  form, on the other hand, H(1) atom of the OH group is maximally displaced from the benzene ring plane (0.32 Å) while N, O(2), O(3) and O(1) atoms exhibit small displacements of 0.05, 0.04, 0.09 and 0.03 Å, respectively.

The C—C—O bond angles in *p*-nitrophenol are not equal (see Fig. 1), a feature common to many other phenolic compounds. This inequality is considered to be due to the bent orbitals resulting from repulsion between hydrogen atom and carbon carrying the hydroxyl group. We observe some differences between  $\beta$  and  $\alpha$  forms of *p*-nitrophenol in relation to this inequality. The value is 6.24° for  $\beta$  form and 5.5° for  $\alpha$  form. The C—C—N bond angles show small dif-

**Table III**  
Hydrogen bond critical points

Bond	Bond length	Hessian eigenvalues			$\rho$ (eÅ <sup>-3</sup> )	$\nabla^2\rho$ (eÅ <sup>-5</sup> )
		$\lambda_1$	$\lambda_2$	$\lambda_3$		
<i><math>\beta</math></i>						
O(2)···H(2 <sup>a</sup> )	2.382(1)	-0.44	-0.27	1.80	0.076(14)	1.147(10)
O(3)···H(1 <sup>a</sup> )	1.909(1)	-0.71	-0.45	5.82	0.11(3)	4.66(5)
O(1)···H(3 <sup>b</sup> )	2.345(1)	-0.25	-0.24	1.14	0.039(13)	0.66(1)
O(2)···H(5 <sup>c</sup> )	2.400(1)	-0.08	-0.05	0.38	0.007(8)	0.257(4)
Symmetry codes: a) $x-1/2, -y+1/2+1, z+1/2$ ; b) $-x+1/2, y-1/2, -x+1/2+1$ ; c) $-x-1, -y+1, -z+2$						
<i><math>\alpha</math></i>						
O(2)···H(1 <sup>a</sup> )	2.461(1)	-0.10	0.08	0.92	0.016(13)	0.897(8)
O(3)···H(1 <sup>a</sup> )	1.890(1)	-1.35	-1.11	4.89	0.19(3)	2.43(4)
N···H(1 <sup>a</sup> )	2.467(1)	-0.10	0.08	0.92	0.016(13)	0.897(8)
O(1)···H(2 <sup>b</sup> )	2.509(1)	-0.12	-0.06	0.99	0.029(9)	0.814(6)
O(3)···H(3 <sup>c</sup> )	2.617(1)	-0.12	-0.11	0.80	0.035(5)	0.562(2)
O(2)···H(5 <sup>d</sup> )	2.406(1)	-0.18	-0.12	1.19	0.040(10)	0.890(9)
<b>Irradiated <math>\alpha</math></b>						
O(2)···H(1 <sup>a</sup> )	2.466(2)	-0.10	0.08	0.75	0.03(1)	0.946(1)
O(3)···H(1 <sup>a</sup> )	1.881(1)	-1.38	-1.04	4.28	0.11(4)	3.07(3)
N···H(1 <sup>a</sup> )	2.466(1)	-0.10	0.08	0.75	0.03(1)	0.948(1)
O(1)···H(2 <sup>b</sup> )	2.498(1)	-0.10	-0.06	1.00	0.039(9)	0.804(2)
O(3)···H(3 <sup>c</sup> )	2.603(1)	-0.12	-0.07	0.72	0.030(4)	0.499(2)
O(2)···H(5 <sup>d</sup> )	2.392(1)	-0.21	-0.12	1.21	0.018(7)	0.600(3)

Symmetry codes: a)  $x+1, -y+1/2, z+1/2$ ; b)  $-x, y-1/2, -z-1/2$ ; c)  $-x+1, -z$ ; d)  $-x+2, -y, -z$

ferences. Furthermore, the N—O(3) bond is slightly longer by 0.01 Å in  $\alpha$  form, compared to  $\beta$  form.

**Table IV**  
Pseudoatomic charges and dipole moments

Atom	$\beta$	$\alpha$	irradiated $\alpha$
O(1)	-0.09(9)	-0.29(10)	-0.08(7)
O(2)	-0.14(9)	-0.36(10)	-0.10(8)
O(3)	-0.22(9)	-0.30(10)	-0.04(9)
N	-0.47(21)	-0.60(22)	-0.25(20)
C(1)	0.00(13)	0.29(13)	-0.06(8)
C(2)	-0.01(12)	0.32(12)	-0.08(7)
C(3)	-0.08(13)	0.30(13)	-0.15(7)
C(4)	-0.49(13)	0.21(11)	0.00(7)
C(5)	-0.06(12)	0.20(13)	-0.13(7)
C(6)	-0.10(12)	0.30(12)	0.04(7)
H(1)	0.46(6)	0.03(11)	0.33(6)
H(2)	0.32(7)	0.03(11)	0.11(5)
H(3)	0.30(7)	-0.02(11)	0.20(5)
H(5)	0.30(7)	-0.06(11)	0.11(5)
H(6)	0.27(8)	0.02(10)	0.12(5)
Dipole moment (Debye)	21.5	18.0	9.9

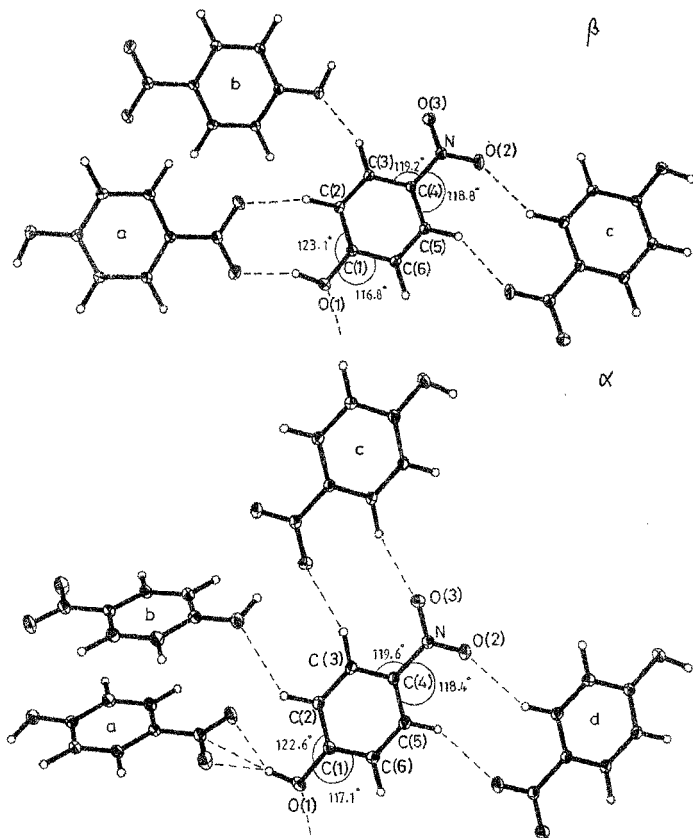


FIG. 1. Molecular packing diagrams of the  $\beta$  and  $\alpha$  polymorphs of *p*-nitrophenol.

The crystal packing in  $\beta$  and  $\alpha$  modifications is noticeably different.  $\beta$  form crystallizes in  $P2_1/n$  space group with the cell dimensions of  $a = 3.6812(3)$ ,  $b = 11.152(9)$ ,  $c = 14.6449(12)$  Å and  $\beta = 92.804(2)^\circ$ . We find no orientational relation of this cell with that of  $\alpha$  form, which occurs in  $P2_1/c$  space group with  $a = 6.1664(1)$ ,  $b = 8.8366(3)$ ,  $c = 11.5435(4)$  Å and

$\beta = 103.390(1)^\circ$ . Obviously, the approach of the adjacent molecules is different in the two structures. The adjacent nonparallel molecules subtend an angle of  $74.73^\circ$  in  $\alpha$  form, but they tend to align nearly parallelly in  $\beta$  form ( $29.26^\circ$ ).

The differences in crystal packing between  $\beta$  and  $\alpha$  forms are reflected in the intermolecular hydrogen bonds (see Fig. 1 and Table III). In  $\beta$  structure, there are two nearly parallel H-bonds originating from nitro-oxygens apart from four other bonds involving phenyl hydrogens. In  $\alpha$  form, as many as nine hydrogen contacts can be predicted. In both the forms, the O(3)...H(1) contact at  $\sim 1.9 \text{ \AA}$ , with an O(3)...H(1)—O(1) angle greater than  $160^\circ$  appears to be the strongest. It is interesting to note that H(1) interacts with the entire nitro group in  $\alpha$  structure and it is possible that the stability of  $\alpha$  structure is related to such favorable hydrogen bonding in the intermolecular region. Charge density analysis throws light on this aspect as will be seen later.

### 3.2. Charge density analysis

We shall first examine intramolecular bonding in the two modifications of *p*-nitrophenol. The residual density maps, obtained as the difference between calculated and experimental densities, were featureless, the magnitude of the random peaks being less than  $0.12 \text{ e\AA}^{-3}$ . The static deformation density,  $\Delta\rho$ , obtained as the difference between total and spherical densities without thermal smearing, and the maps are shown in Fig. 2 in the plane of the benzene ring. In both  $\beta$  and  $\alpha$  polymorphs, the deformation density builds up as concentric contours in the regions of C—C bonds of the benzene ring, C—N bond, N—O bonds of the nitro group as well as in C—O and O—H bonds of the hydroxyl group. The lone-pair electrons of the oxygen atoms are also clearly seen in Fig. 2. In order to be able to quantitatively compare the two charge densities in the polymorphs, we have carried out CP search along different bonds. Regardless of the crystal form, the intramolecular CPs are of (3,−1) type with negative Laplacians, charac-

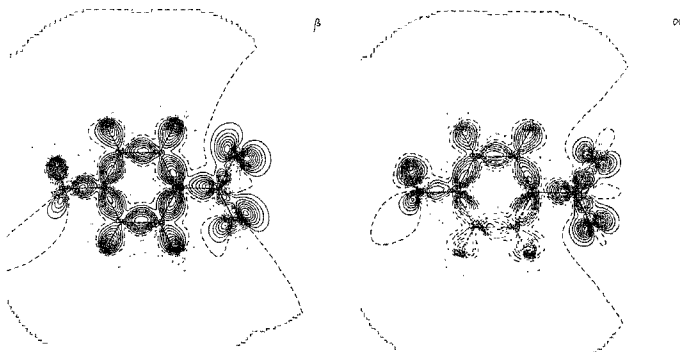


FIG. 2. Static deformation density in the plane of the benzene ring for  $\beta$  and  $\alpha$  forms of *p*-nitrophenol. Contour intervals at  $0.1 \text{ e\AA}^{-3}$ .

teristic of a covalently bonded molecular system. In Table III, we list the bond critical points of  $\beta$  and  $\alpha$  forms obtained from the present analysis.

The electron densities at the CPs,  $\rho_{CP}$ , of the six C—C bonds in the benzene ring vary in a rather narrow range, 2.2–2.35 eÅ<sup>-3</sup> for  $\beta$  form and 2.01–2.20 eÅ<sup>-3</sup> for  $\alpha$  form, with mean values of 2.26 and 2.09 eÅ<sup>-3</sup>, respectively. The mean values of the Laplacians,  $\nabla^2\rho_{CP}$ , are -22.83 and -18.28 eÅ<sup>-5</sup>. Following Cremer and Kraka,<sup>23</sup>  $\rho_{CP}$  and  $\nabla^2\rho_{CP}$  values correspond to mean bond orders of 2.02 and 1.70 in  $\beta$  and  $\alpha$  forms, respectively, akin to those in aromatic rings. The ellipticity,  $\epsilon$ , in both the forms is somewhat lower than the theoretical value of 0.33. These homonuclear bonds are polarized a little, some up to 12% due to perturbation caused by the two functional groups. The mean densities in the C—H bond regions of the benzene rings of the two forms are similar (~1.9 eÅ<sup>-3</sup>) and are close to the theoretical density of 1.846 eÅ<sup>-3</sup>; the Laplacians are ~-18.8 and -19.8 eÅ<sup>-5</sup> for  $\beta$  and  $\alpha$  forms, respectively. The polarity of C—H bonds,  $\Delta$ , is expected to be 26.6% towards hydrogen and we obtain mean  $\Delta$  values close to 21% in the two forms.

The C(1)—O(1) bond connecting the hydroxyl group to the benzene ring is associated with  $\rho_{CP}$  values of 2.32 and 2.09 eÅ<sup>-3</sup> for  $\beta$  and  $\alpha$  forms, respectively. The corresponding bond orders are 1.43 and 1.23. The bond is polarized towards C(1), with  $\Delta = 35.4\%$  for  $\beta$  modification (theoretical value ~35%) and a lower value of 22.9% for  $\alpha$  modification. The O(1)—H(1) bond region also exhibits some differences. In this case,  $\rho_{CP}$  value in  $\beta$  form is lower than that in  $\alpha$  form by 0.23 eÅ<sup>-3</sup>. Interestingly, however, CPs in the C(1)—O(1)—H(1) region deviate significantly ( $d \sim 0.03$  Å) from the intermolecular vectors due to bending of orbitals (see Table II), which is also reflected in the inequality of C—C—O bond angles.

The C(4)—N bond linking the nitro group to the benzene ring is associated with  $\rho_{CP}$  values of 1.91 and 1.78 eÅ<sup>-3</sup> in  $\beta$  and  $\alpha$  forms, respectively, and with the corresponding bond orders of 1.03 and 0.93. The bonding within the nitro group varies from one polymorph to the other and also between the two N—O bonds of the nitro group. The  $\beta$  form exhibits  $\rho_{CP}$  values of 3.14 and 3.03 eÅ<sup>-3</sup> for the N—O(2) and N—O(3) bonds, respectively, while the  $\alpha$  form shows much higher densities of 3.49 and 3.39 eÅ<sup>-3</sup> for the same bonds, the latter being close to that expected for a double bond. The ellipticity of N—O(3) bonds in both the forms is somewhat larger than that of N—O(2) bonds. The Laplacians and the bond polarities of N—O bonds are low in both the forms, possibly because of the presence of intermolecular hydrogen bonding.

From the above comparison of charge densities of  $\beta$  and  $\alpha$  forms, it appears that density migrates outwardly from the benzene ring of the molecule to nitro and hydroxyl groups when the crystal structure changes from  $\beta$  to  $\alpha$ . Accordingly, the group charges of NO<sub>2</sub> are -0.83 and -1.26 in  $\beta$  and  $\alpha$  forms, respectively, and of OH are 0.37 and -0.26, respectively. In Table IV, we list the pseudoatom charges in the two forms. The calculated molecular dipole moments in the two forms differ to some extent (Table IV), but both the values are considerably larger than in the free molecule. The experimental value of dipole moment of the free molecule<sup>24</sup> as well as that calculated by us<sup>25</sup> is around 5.5 Debye. This enhancement of the dipole moment clearly arises from the charge densities in the condensed state and is in line with the observation of Howard *et al.* for 2-methyl 4-nitroaniline.<sup>12</sup>

The lone-pair electrons on the oxygen atoms of the nitro group occur as (3, -3) critical points in deformation density<sup>1,2</sup> and show significant differences between the two forms. The mean density of the lone pairs is  $\sim 5.5 \text{ e}\text{\AA}^{-3}$  in  $\beta$  form, much smaller than that in  $\alpha$  form ( $\sim 7.6 \text{ e}\text{\AA}^{-3}$ ).<sup>2</sup> We also notice that the lone-pair lobes are slightly closer to the nucleus in  $\alpha$  form ( $\sim 0.29 \text{ \AA}$ ) as compared to  $\beta$  form ( $\sim 0.39 \text{ \AA}$ ). Our later discussion of the intermolecular hydrogen bonding will bring this issue in right perspective.

Hydrogen bonding between one of the oxygens of the nitro group and the hydroxyl hydrogen of the adjacent molecule (O(3)...H(1)) is the shortest intermolecular contact ( $\sim 1.9 \text{ \AA}$ ) in both the forms. Charge density analysis reveals the presence of bond critical points with small densities, 0.11 and  $0.19 \text{ e}\text{\AA}^{-3}$  for  $\beta$  and  $\alpha$  forms, respectively. The Laplacians at the CPs are also small and positive. These observations imply a closed shell interaction in intermolecular hydrogen bonding.<sup>2</sup> Apart from the O(3)...H(1) contact, we have analysed other hydrogen contacts as well. These are weak interactions as seen from the  $\rho_{\text{CP}}$  and  $\nabla^2\rho$  values listed in Table III. The two polymorphs exhibit some differences in weak hydrogen bonds, the number of weak contacts being five and eight in  $\beta$  and  $\alpha$  forms, respectively. The O(2)...H(2) contact in  $\beta$  form is nearly parallel to the main hydrogen bond (see Fig. 1) and exhibits a moderate density ( $0.076 \text{ e}\text{\AA}^{-3}$ ) compared to the other weak contacts. An interesting feature in  $\alpha$  structure is that a common critical point is present with a density of  $\sim 0.016 \text{ e}\text{\AA}^{-3}$  for the N...H(1) and O(2)...H(1) contacts, providing evidence for the participation of the entire nitro group in hydrogen bonding.

The variations observed in the intermolecular hydrogen bonding region involving nitro group are best represented using relief maps of the negative Laplacian.<sup>2</sup> We show such maps in Fig. 3 for both the polymorphs in the plane of the oxygen atoms of nitro and hydroxyl groups involved in intermolecular bonding. We see from the figure that the oxygen lone-pair lobes are polarized in the direction of the hydrogen atom in both the cases. A major difference between the two forms is that the hydroxyl group appears to have rotated and moved closer to nitro group in  $\alpha$  form and that hydrogen is now more closer to the plane formed by oxygen atoms as seen from the increase in the intensity of hydrogen peak in the map. The conclusions derived

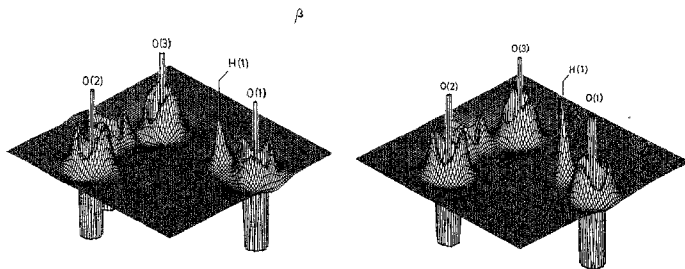


FIG. 3. Relief map of the negative Laplacian in the plane of the hydrogen bond. Range,  $-250$  to  $250 \text{ e}\text{\AA}^{-5}$ .

from the geometrical structure and critical points of the intermolecular charge distribution are thus substantiated using relief maps.

### 3.3. Effect of irradiation of $\alpha$ form

We have investigated the geometrical structure and the topography of charge distribution of  $\alpha$  form after irradiation. Surprisingly, the geometrical structure showed little variation following irradiation in sunlight for several days, although the change in color from yellow to deep red was striking. Charge density analysis however revealed important differences. In Fig. 4(a) we show the static deformation density in the plane of benzene ring for the irradiated  $\alpha$  form. A comparison of Fig. 2 and 4(a) shows that the deformation density of the irradiated  $\alpha$  form differs from the pristine form and resembles closely that of  $\beta$  form. We have analysed this aspect carefully using CP search (see Table II).

The mean value of C—C bonds of the benzene ring in the irradiated form is  $2.13 \text{ e}\text{\AA}^{-3}$  corresponding to a bond order of 1.77. This value may be compared with that obtained before irradiation (1.70) and also that of  $\beta$  form (2.02). The mean density in C—H bond regions of the benzene ring is very similar to those obtained with the two polymorphs ( $\sim 1.9 \text{ e}\text{\AA}^{-3}$ ). The C(1)—O(1) bond exhibits bond order of 1.25 slightly higher than that in pristine form. The O(1)—H(1) bond region exhibits noticeable differences. The  $\rho_{\text{CP}}$  value in  $\alpha$  form decreases remarkably upon irradiation from 2.91 to  $2.40 \text{ e}\text{\AA}^{-3}$ . The  $\beta$  form exhibits a moderate density of  $2.68 \text{ e}\text{\AA}^{-3}$ . The C(4)—N bond linking nitro group to the benzene ring in  $\alpha$  form remains essentially unchanged on irradiation (bond order  $\sim 0.94$ ) though bonding within the nitro group varies significantly. The irradiated crystal exhibits moderate densities of 3.15 and  $3.18 \text{ e}\text{\AA}^{-3}$  in N—O(2) and N—O(3) bond regions, respectively, as compared to pristine  $\alpha$  (3.49 and  $3.39 \text{ e}\text{\AA}^{-3}$ , respectively) and  $\beta$  forms (3.14 and  $3.03 \text{ e}\text{\AA}^{-3}$ , respectively). We notice from Table II that some of the Laplacians in the nitro group are small positive numbers in contrast to the negative values observed in general for covalently bonded systems. This may be due to higher ionicity of the nitro bonds.

Following irradiation, noticeable changes take place in intermolecular hydrogen bonding. The density with the shortest contact (O(3) $\cdots$ H(1)) decreases from 0.19 to  $0.11 \text{ e}\text{\AA}^{-3}$  and is similar to that obtained for the same contact in  $\beta$  form. There are some differences in weaker contacts as well (see Table III). The density at the common critical point of N $\cdots$ H(1) and O(2) $\cdots$ H(1) contacts increases marginally after irradiation. We find that the relief map of the negative Laplacian shown in Fig. 4b resembles that of pristine  $\alpha$  form in that the hydroxyl group appears to have rotated and moved closer to nitro group compared to the situation in  $\beta$  form. However, the lone-pair polarization as well as the magnitude of the hydrogen peak is much less, similar to  $\beta$  form.

From Table IV, we obtain the group charges of NO<sub>2</sub> and OH of the irradiated crystal to be  $-0.39$  and  $0.25$ , respectively. These values are quite different from those found before irradiation ( $-1.26$  and  $-0.26$ , respectively) as well as from those of  $\beta$  form ( $-0.83$  and  $0.37$  respectively). Charge distribution appears to be less polarized after irradiation. As a result, molecular dipole moment is relatively low in the irradiated crystal (9.9 Debye, see Table IV).

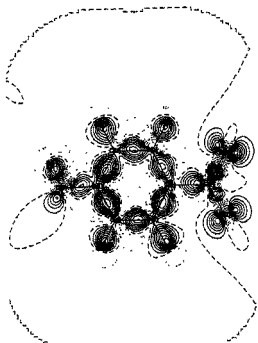


FIG. 4(a). Static deformation density in the plane of the benzene ring for the irradiated  $\alpha$  form. Contour intervals at  $0.1 \text{ e}\text{\AA}^{-3}$ .

(a)

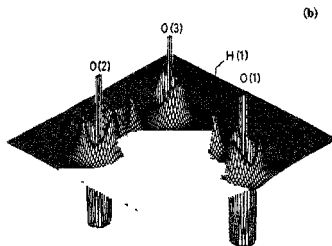


FIG. 4(b) Relief map of the negative Laplacian in the plane of the hydrogen bond. Range,  $-250$  to  $250 \text{ e}\text{\AA}^{-5}$ .

(b)

The lone-pair electrons on the oxygen atoms of the nitro group show significant differences among the three cases. The mean total density at lone-pair CPs is  $\sim 6.97 \text{ e}\text{\AA}^{-3}$  in the irradiated crystal compared to  $\sim 7.6 \text{ e}\text{\AA}^{-3}$  and  $\sim 5.5 \text{ e}\text{\AA}^{-3}$  in pristine  $\alpha$  and  $\beta$  forms, respectively. We also find that the lone-pair lobes move slightly closer to the nucleus after irradiation by  $\sim 0.02 \text{ \AA}$ .

#### 4. Conclusions

The main conclusions from the present study are as follows:

- (i) The  $\alpha$  form exhibits greater number of intermolecular hydrogen bonds compared to  $\beta$  form which accounts for its thermodynamic stability. The presence of a common CP in the intermolecular region provides a favourable hydrogen bonding in  $\alpha$  form.
- (ii) The  $\alpha$  form retains its geometrical structure even after prolonged irradiation, but undergoes subtle changes in the topography of molecular charge density resembling somewhat like that found in the light stable  $\beta$  form.
- (iii) The charge appears to migrate outwardly from benzene ring to nitro and hydroxyl groups when the crystal structure changes from  $\beta$  to  $\alpha$ . On irradiation, the charge migrates inwardly and the distribution becomes more even across the whole molecule accompanying photochemical transition. The dipole moment is also much smaller (9.9 Debye).

#### Acknowledgement

The author enjoys collaborating with Prof. C. N. R. Rao, F. R. S., and is also grateful to him for encouragement. The presentation is based on some recent publications and the contributions of Dr P. Kumaradhas and Mr Srinivasa Gopalan are duly acknowledged.

## References

1. COPPENS, P. *X-ray charge densities and chemical bonding*, Oxford Univ. Press, 1997.
2. JEFFREY, G. A. AND PINIELLA, J. F. *The application of charge density research to chemistry and drug design*, Plenum Press, 1991.
3. HANSEN, N. K. AND COPPENS, P. Electro population analysis of accurate diffraction data, *Acta Cryst.*, 1978, **34**, 909–914.
4. BADER, R. F. W. *Atoms in molecules—a quantum theory*, Clarendon Press, 1990.
5. WOZNIAK, K., HE, H., KLIJNOWSKI, J., JONES, W. AND GRECH, E. Attractive inter- and intramolecular N...O interactions in N, N-dipicrylamine and its ionic complexes, *J. Phys. Chem.*, 1994, **98**, 13755–13765.
6. MALLINSON, P. R., WOZNIAK, K., GARRY, T. AND MCCORMACK, K. L. A charge density analysis of cationic and anionic hydrogen bonds in a 'proton sponge', *J. Am. Chem. Soc.*, 1997, **119**, 11502–11509.
7. MADSEN, D., FLENSBURG, C. AND LARSEN, S. Properties of the experimental charge density of thylammonium hydrogen maleate, a salt with a very short intramolecular O—H—O hydrogen bond, *J. Phys. Chem. A*, 1998, **102**, 2177–2188.
8. HOWARD, S. T., HURSTHOUSE, M. B., LEHMANN, C. W. AND POYNER, E. A. Experimental and theoretical determination of electronic properties in L-dopa, *Acta Cryst. B*, 1995, **51**, 328–337.
9. MILANESIO, M., BIANCHI, R., UGLIENGO, P. AND VITERBO, D. Vitamin C at 120 K: experimental and theoretical study of the charge density, *Theochem*, 1997, **419**, 139–154.
10. FLAIG, R., KORITSANSZKY, T., ZOBEL, D. AND LUGER, P. Topological analysis of the experimental electron densities of amino acids. 1. DL-Aspartic acid at 20 K, *J. Am. Chem. Soc.*, 1998, **120**, 2227–2238.
11. HAMZAOU, F., BRET, F. AND WOJCIK, G. Electron-density study of *m*-nitrophenol in the orthorhombic structure, *Acta Cryst. B*, 1996, **52**, 159–164.
12. HOWARD, S. T., HURSTHOUSE, M. B., LEHMANN, C. W., MALLINSON, P. R. AND FRAMPTON, C. S. Experimental and theoretical study of the charge density in 2-methy-4-nitroaniline, *J. Chem. Phys.*, 1992, **97**, 5616–5630.
13. COPPENS, P., FOMITCHEV, D. V., CARDUCCI, M. D. AND CULP, K. Crystallography of molecular excited states. Transition-metal nitrosyl complexes and the study of transient species, *J. Chem. Soc. Dalton Trans.*, 1998, 865–872.
14. KULKARNI, G. U., KUMARDHAS, P. AND RAO, C. N. R. Charge density study of the polymorphs of *p*-nitrophenol, *Chem. Mater.*, 1998, **10**, 3498–3505.
15. KUMARDHAS, P., GOPALAN, R. S. AND KULKARNI, G. U. A charge density study of the effect of irradiation on the  $\alpha$ -form of *p*-nitrophenol, *Proc. Indian Acad. Sci. Chem. Sci.* (in print).
16. COPPENS, P. AND SCHMIDT, G. M. J. The crystal structure of the metastable ( $\beta$ ) modification of *p*-nitrophenol, *Acta Cryst.*, 1965, **18**, 654–663.
17. COPPENS, P. AND SCHMIDT, G. M. J. X-ray diffraction analysis of *o*-nitrobenzaldehydes, *Acta Cryst.*, 1964, **17**, 222–226.
18. ATHERTON, N. M., HEATH, J. P., SHOHOJI, C. B. AND TORRANCE, C. A. Single-crystal ENDOR study of  $\gamma$ -irradiated *p*-nitrophenol, *J. Chem. Soc. Faraday Trans.*, 1990, **86**, 3197–3200.
19. *Users manual*, Siemens Analytical X-ray Instruments, Inc., Madison, Wisconsin, USA, 1995.

20. SHELXTL (Silicon Graphics version), Siemens Analytical X-ray Instruments Inc, Madison, Wisconsin, USA, 1995.
21. KORITSANSKY, T., HOWARD, S. T., RICHTER, T., MALLINSON, P. R., SU, Z. AND HANSEN, N. K. *XD. A computer program package for multipole refinement and analysis of charge densities from diffraction data*, Internet source: [xd-user@chemie.fu-berlin.de](mailto:xd-user@chemie.fu-berlin.de), 1995.
22. NARADELLI, M. PARST program package, *Comput. Chem.*, 1983, 7, 95–102.
23. CREMER, D. AND KRAKA, E. A description of the chemical bond in terms of local properties of electron density and energy, *Croatica Chim. Acta*, 1984, 57, 1259–1281.
24. WESSON, L. G. *Tables of electric dipole moments*, MIT Press, 1948.
25. STEWART, J. J. P. MOPAC Program, *Quantum Chemistry Program Exchange*, 1990, <http://comp.chem.umn.edu/www.MOPAC>.